Flexible Backhaul-aware DBS-aided HetNet with IBFD Communications

Nirwan Ansari and Liang Zhang*

Advanced Networking Laboratory, Department of Electrical and Computing Engineering,
New Jersey Institute of Technology, Newark, NJ 07102 USA.

Abstract

Drone-mounted base-stations (*DBS*s) are promising complements and substitutes of the terrestrial base-stations. We investigate the problem of Placement and cOmmunications in the DBS-aided heterogeneous network (*POD*) with tier-1 backhaul using free space optics communications and tier-2 backhaul utilizing in-band full-duplex communications to provide ubiquitous connections and high spectrum efficiency. The POD problem is shown to be NP-hard, and thus we simplify the POD problem by decomposing it into three sub-problems. Finally, we propose an approximation algorithm to solve the POD problem, and demonstrate that the proposed algorithm is superior to two baseline algorithms.

Keywords: Drone-mounted base-stations, unmanned aerial vehicles, heterogeneous networks, wireless backhauling, full-duplex, OFDMA, resource allocation.

1. Introduction

There are many challenges to realize 5G networks, i.e., high system capacity (1000× capacity per km^2), high data rates (targeting 1 Gbps per user everywhere and 100× user throughput increase) and massive connectivity (100× connected users) [1, 2]. Many new techniques for communications have been proposed to achieve these goals, and one promising evolution is to leverage emerging techniques such as in-band full-duplex (*IBFD*) to improve the spectrum efficiency [3, 4].

Drone-mounted base-stations (*DBS*s) have the potential to be a promising complement of ground base-stations or even to substitute ground base-stations because of various advantages: robustness against the environmental variation, high flexibility of horizontal relocation, and easy altitude alteration to provide desired quality of service (*QoS*) service [5]. Deploying DBSs to serve user equipments (*UE*s) is an encouraging solution, which can offer ubiquitous connectivity in the next generation wireless networks especially for unexpected incidents or temporary large-scale events, i.e., earthquakes, floods, traffic congestions, and concerts [6]. DBS communications is enabling various emerging applications. For example, Nokia and UK mobile operator created a DBS prototype for 4G LTE network in 2016 [7]; Verizon deployed unmanned aerial vehicles (*UAV*s) to provide LTE service in 2016; ATT raised the Cell Tower on Wings (*COW*) project in order to provide service for emergent or large-scale events; some other projects such as Facebook's Aquila and Google's SkyBender also provided wireless connectivity through UAVs [5].

IBFD communications can potentially double the spectrum efficiency, but it induces self-interference (*SI*) to the receiver, and thus the performance of the spectrum efficiency highly depends on the SI cancellation [8]. SI can be mitigated by the SI cancellation up to 150 *dB* [9]. Bharadia *et al.* [10] designed and implemented an IBFD communications prototype, which provides nearly double throughput. In this paper, we investigate the problem of Placement and cOmmunications in the IBFD DBS-aided HetNet (*POD*) with flexible bandwidth and power assignment in the tier-2 backhaul that has not been investigated.

The main contributions of this article are epitomized as follows: 1) We propose a DBS-aided HetNet framework with IBFD communications for 5G networks, and free space optics (*FSO*) is leveraged to provide connections for the tier-1 backhaul. This framework provisions flexible deployment because all BSs are flyable and FSO links can provide effective communications over a long distance; 2) We have studied the DBS placement, the UE association, and the bandwidth and power assignment in the access links and the tier-2 backhaul links. The access link of a DBS can reuse the frequency spectra of its tier-2 backhaul link; 3) We decompose the POD problem into three sub-problems, and propose approximation algorithms to solve the sub-problems sequentially; 4) We propose an approximation algorithm, named the AA-POD algorithm, to efficiently solve the POD problem with an approximation ratio of $\frac{1}{2}(1-\frac{1}{2^k})$ (k is the number of loops) to obtain the optimal horizontal and vertical positions of DBSs.

The rest of this article is coordinated as follows. Related works are delineated in Section 2, and the system model is introduced in Section 3. The POD problem is formulated in Section 4 and analyzed in Section 5. Then, the evaluation results for the POD problem are summarized in Section 6. Finally, conclusions are drawn in Section 7.

☆This work was supported in part by National Science Foundation under Grant CNS-1814748.

*Corresponding author.

**Email address: nirwan.ansari@njit.edu (Nirwan Ansari); lz284@njit.edu (Liang Zhang)

2. Related Works

DBS communications is increasingly drawing much attention lately. Sekander *et al.* [5] investigated the feasibility of a multi-tier DBS-aided network architecture and evaluated the performance of the downlink spectral efficiency. Al-Hourani *et al.* [11] focused on the altitude optimization by which the maximum coverage of a low altitude platform, i.e., DBS, can be achieved, and they also proposed the radio propagation model for the LAPs. Alzenad *et al.* [12] studied a 3D placement problem of one UAV with the objective to maximize the number of provisioned UEs with various required QoS. Zhao *et al.* [13] studied the UAVs deployment and placement problem in a hot spot area to provide service to unevenly distributed ground UEs with required QoS.

FD communications has been proposed to enhance spectral efficiency. Nam *et al.* [14] investigated the joint subcarrier and power assignment problem in an OFDMA network with one ground base-station, and the objective is to maximize the total throughput of the network. Yu *et al.* [15] proposed an ultra-dense ground base-station aided HetNet with FD communications, and their target is to maximize the total throughput of the network while offering fairness to UEs. Siddique *et al.* [16] considered communications of small BSs (IBFD enabled, out of band enabled or hybrid enabled) overlaid with an macro-cell, and the target is to maximize the minimum data rate of all small BSs (the data rate of a small BS is determined by the access link and the backhaul link). Sharma *et al.* [17] proposed a two-tier HetNet with IBFD-enabled small BSs and HD-enabled macrocells for the downlink and uplink communications, and the target is to maximize the coverage probability and the spectrum efficiency of the network (the coverage probability is the probability of a randomly selected UE with received SINR above a pre-determined SINR threshold). Although there are many works about DBS communications and FD communications separately, but few have addressed DBS-aided HetNet with flexible IBFD backhaul communications.

3. System Model

Fig. 1 shows a DBS-assisted HetNet frequency division duplex (*FDD*) OFDMA framework. All DBSs are FD-enabled while the mother DBS (*MDBS*) and all UEs are HD-enabled. The MDBS includes one portable BS, one access switch, one Ethernet converter (FSO/Ethernet signal conversion), one FSO transceiver and a powerful battery. Since the cost of the MDBS is high (including a powerful DBS, an FSO terminal and other equipments), the FSO terminal is only equipped with the MDBS. An access link is the connection between the DBS and a UE; a tier-2 backhaul link is the connection between the DBS and the MDBS; the tier-1 backhaul link is the connection between the MDBS and the core network, which employs FSO for communications. The same frequency spectrum is utilized to transmit data in the tier-2 backhaul link and the access link of a DBS.

In Fig. 1, each UE is provisioned by one BS, different DBSs use different frequency spectra, and different UEs utilize different frequency spectra to avoid UE-UE interference. In the

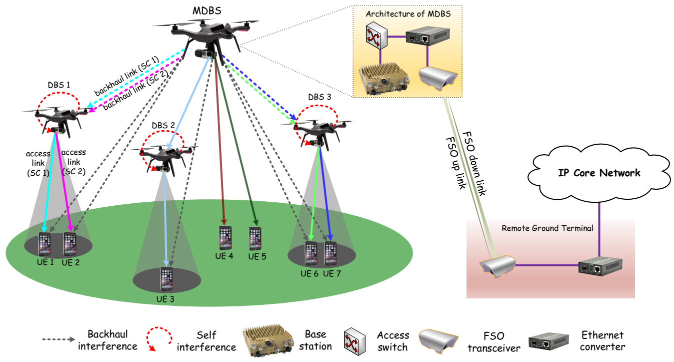

Figure 1: Full duplex enabled DBS-aided HetNet framework.

FDD OFDMA network, each UE can be assigned with one or more sub-channels (*SC*) (viz., resource blocks) while one SC can accommodate at most one UE. For example, UE 1 is assigned with SC 1 while UE 2 is assigned with SC 2; the tier-2 backhaul link (MDBS-DBS 1) also uses SC 1 and SC 2 for the transmission; FSO links are utilized to communicate between the remote ground terminal and the MDBS. Here, each UE suffers the backhaul interference from the MDBS and each DBS is inflicted by SI.

3.1. BS-UE Channel Model

Two types of pass loss are considered in Fig. 1: air-to-ground (*A2G*) path loss (DBS-UE or MDBS-UE) and air-to-air (*A2A*) path loss (MDBS-DBS). The A2G path loss includes line-of-sight (*LoS*) and none-line-of-sight (*NLoS*) path loss [11]. The probabilities of an A2G link experiencing LoS ($\phi^L_{i,j}$) and NLoS ($\phi^N_{i,j}$) between the ith UE and the jth DBS are expressed as [18]:

$$\begin{cases} \phi^L_{i,j} = [1 + a \cdot exp(-b(\frac{180\theta_{i,j}}{\pi} - a))]^{-1}, \\ \phi^N_{i,j} = 1 - \phi^L_{i,j}. \end{cases} \tag{1}$$

Here, $\theta_{i,j} = arctan(\frac{h_j}{\zeta_{i,j}})$ is the elevation angle, $\zeta_{i,j}$ is the 3-D distance between the ith UE and the jth DBS, h_j is the altitude of the jth DBS, and a and b are environment parameters, i.e., suburban, urban, dense urban, and high-rise urban, respectively [12, 11]. The path loss of the LoS ($\gamma^L_{i,j}$) and that of NLoS ($\gamma^N_{i,j}$) between the ith UE and the jth DBS are

$$\begin{cases} \gamma^L_{i,j} = \eta^L_1 + \eta^L_2 log_{10}(\zeta_{i,j}), \\ \gamma^N_{i,j} = \eta^N_1 + \eta^N_2 log_{10}(\zeta_{i,j}). \end{cases} \tag{2}$$

Here, η^L_1 and η^N_1 are the fixed path loss for LoS and NLoS, respectively; η^L_2 and η^N_2 are exponents path loss experiencing LoS and NLoS connections, respectively [19, 20]. Then, $\gamma_{i,j}(h, \zeta)$, the path loss between the ith UE and the jth DBS is

$$\begin{aligned} \gamma_{i,j}(h, \zeta) &= \phi^L_{i,j}\gamma^L_{i,j} + \phi^N_{i,j}\gamma^N_{i,j} \\ &= \eta^N_1 + \eta^N_2 log_{10}(\zeta_{i,j}) + \phi^L_{i,j}[\beta_1 + \beta_2 log_{10}(\zeta_{i,j})]. \end{aligned} \tag{3}$$

Here, $\beta_1 = \eta^L_1 - \eta^N_1$ and $\beta_2 = \eta^L_2 - \eta^N_2$. Obviously, the A2A path loss is determined by the 3-D distance between the DBS and the UE and the altitude of the DBS.

3.2. MDBS-DBS Channel Model

Let Γ_j be the path loss from the MDBS to the jth DBS, as expressed in Eq. (4). Here, only the free-space path loss is considered because the link between two UAVs are dominated by the LoS connections [13]; $\tilde{\zeta}_{1,j}$ is the 3-D distance between the jth DBS and the MDBS; f_0 is the carrier frequency and c_0 is the speed of light.

$$\Gamma_j = 20log(\frac{4\pi f_0 \tilde{\zeta}_{1,j}}{c_0}), \quad \forall j \in \mathcal{B}. \tag{4}$$

3.3. Communication Model

We focus on downlink communications in the proposed framework (UEs receive data from the MDBS or DBSs), and assume each UE is provisioned by one BS. Let $d_{i,j}$ and $s_{i,j}$ be the data rate and the signal to interference plus noise ratio (*SINR*) of the ith UE when it is assigned to the jth BS, as expressed in Eqs. (5)-(6). Here, $\widetilde{b}_{i,j}$ and $p_{i,j}$ are the assigned bandwidth and power for the ith UE by the jth BS ($b_{i,j}$ is the assigned bandwidth in terms of SCs, $b_{i,j} = \lceil \widetilde{b}_{i,j}/b_0 \rceil$); $\breve{p}_{i,1}$ is the tier-2 backhaul interference power to the ith UE from the MDBS; $\gamma_{i,1}$ is the channel gain from the MDBS to the ith UE and $\sigma^2_{i,j}$ is the thermal noise power.

$$d_{i,j} = \widetilde{b}_{i,j} log_2(1 + s_{i,j}), \quad \forall i \in \mathcal{U}, j \in \mathcal{B}. \tag{5}$$

$$s_{i,j} = \begin{cases} \frac{p_{i,j}\gamma_{i,j}}{\sigma^2_{i,j}}, & \forall i \in \mathcal{U}, j = 1, \\ \frac{p_{i,j}\gamma_{i,j}}{\breve{p}_{i,1}\gamma_{i,1} + \sigma^2_{i,j}}, & \forall i \in \mathcal{U}, j \in \mathcal{B}, j > 1. \end{cases} \tag{6}$$

Let ξ_j be the data rate of the tier-2 backhaul link of the jth DBS:

$$\xi_j = \tilde{f}_j log_2(1 + \frac{P_j \Gamma_j}{\tilde{\beta}_j + \sigma^2_j}), \quad j \in \mathcal{B}, j > 1, \tag{7}$$

where $\tilde{f}_j$ and P_j are the assigned bandwidth and power for the tier-2 backhaul link of the jth DBS; $\sigma^2_j = \tilde{f}_j N_0$ is the thermal noise power and N_0 is the thermal noise power spectral density; $\tilde{\beta}_j = \frac{1}{\tilde{\beta}_{SI}} \sum_i p_{i,j}$ is the SI of the jth DBS and $\tilde{\beta}_{SI}$ is the SI cancellation capability [21].

4. Problem formulation

Let $\mathcal{B}$ be the set of BSs and $\mathcal{U}$ be set of UEs. Let $\omega_{i,j}$ be the UE-BS indicator, and it is 1 if the ith UE is associated with the jth BS; otherwise, it is 0. Let $\tilde{f}_j$ be the total bandwidth from the MDBS to the jth BS, and $\tilde{f}_j = b_0 f_j$. Assume the number of required DBSs is known *a priori* and one MDBS is used. Various variables and notations are summarized in Table 1.

The POD problem is formulated as follows:

Table 1: Notations and Variables

Symbol	Definiton
$\mathcal{B}$	The set of BSs (including the MDBS and DBSs).
$B = \lvert\mathcal{B}\rvert$	The number of all BSs.
Λ_1	The set of candidate locations in the horizontal plane.
Λ_2	The set of candidate locations in the vertical plane.
b_0	The bandwidth of a SC.
d_i	The data rate requirement of the ith UE.
P^{max}_j	The power capacity of the jth BS.
P_j	The transmission power from the MDBS to the jth DBS.
z^k_j	The power-spectral-density of the jth BS in the kth iteration.
ξ_j	The data rate of the tier-2 backhaul link of the jth DBS.
ξ^{fso}	The data rate capacity of the FSO link from the ground terminal to the MDBS.
f^{max}	The total available bandwidth in terms of SCs.
f_j	The total used bandwidth in term of SCs for the jth BS.
$\omega_{i,j}$	The UE-BS indicator.
$p_{i,j}$	The assigned power by the jth BS towards the ith UE.
$b_{i,j}$	The assigned SCs by the jth BS towards the ith UE.
τ_j	The horizontal location of the jth BS, $z_j \in \Lambda_1$.
h_j	The vertical location of the jth BS, $h_j \in \Lambda_2$.
$r_{i,j}$	The achieved data rate of the ith UE towards the jth DBS.

$$\begin{aligned}
\mathscr{P}_0 : & \max_{\omega_{i,j}, p_{i,j}, b_{i,j}, f_j, P_j, \tau_j, h_j} \sum_i \sum_j r_{i,j} \\
s.t. : & \\
& C1 : \sum_j \omega_{i,j} \leq 1, \quad \forall i \in \mathcal{U}, \\
& C2 : \sum_i \omega_{i,j} b_{i,j} \leq f_j, \quad \forall i \in \mathcal{U}, j \in \mathcal{B}, \\
& C3 : \sum_i \sum_j \omega_{i,j} b_{i,j} \leq f^{max}, \\
& C4 : \sum_i \omega_{i,j} p_{i,j} \leq P^{max}_j, \quad j \in \mathcal{B}, j > 1, \\
& C5 : \sum_{j>1} P_j + \sum_i \omega_{i,1} p_{i,1} \leq P^{max}_1, \\
& C6 : \sum_i r_{i,j} \leq \xi_j, \quad \forall i \in \mathcal{U}, j \in \mathcal{B}, j > 1, \\
& C7 : \omega_{i,j} \in \{0, 1\}, \quad \forall i \in \mathcal{U}, j \in \mathcal{B} \\
& C8 : r_{i,j} = \omega_{i,j} d_i, \quad \forall i \in \mathcal{U}, j \in \mathcal{B}, \\
& C9 : \sum_i \sum_j r_{i,j} \leq \xi^{fso}, \\
& C10 : \tau_j \in \Lambda, \quad \forall j \in \mathcal{B}, j > 1. \\
& C11 : h_j \in \Theta, \quad \forall j \in \mathcal{B}, j > 1.
\end{aligned} \tag{8}$$

The objective is to maximize the total throughput of the network, and the problem $\mathscr{P}_0$ includes the following constraints: UE provisioning constraints (C1, C7), the bandwidth capacity constraints (C2, C3), the power capacity constraints (C4, C5), the data rate capacity constraint of the tier-2 backhaul (C6), the data rate capacity constraint of the tier-1 backhaul (C8, C9), and the DBS placement constraints (C10, C11). C1 and C7 ensure that each UE is assigned to at most one BS. C2-C3 impose the total used SCs not to exceed the total available SCs in the network. C4-C5 ensure the total used power of a BS not to exceed its power capacity. C6 and C8 impose the total achieved data rate of all UEs towards a DBS not to exceed the data rate of tier-2 backhaul, and C9 ensures the total achieved data rate of all UEs not to exceed the data rate of tier-1 backhaul. C10-C11 impose all DBSs to be placed within candidate horizontal positions and vertical positions.

5. Problem Analysis

The Maximum profit Generalized Assignment Problem (*Max-GAP*) [22] is a well known NP-hard problem, and any instances of the Max-GAP problem can be reduced into the POD problem (a BS can be mapped into a knapsack, a UE can be mapped into an item, the UE requirement can be mapped into the cost and the data rate of a UE can be mapped into profit) for a given tier-2 backhaul bandwidth and power assignment (i.e., $f_j = f^{max} \cdot B^{-1}$, $P_j = P_j^{max} \cdot B^{-1}$). Thus, the POD problem is NP-hard. To solve the POD problem, we decompose the POD problem into three sub-problems: the DBS Placement problem ($\mathscr{P}_1$), the Bandwidth and powEr AllocaTion (*BEAT*) problem ($\mathscr{P}_2$, bandwidth and power assignment in the tier-2 backhaul links), and the Joint UE assignment, baNdwidth and powEr assignment (*JUNE*) problem ($\mathscr{P}_3$). The sub-problems are solved one by one, and then an approximation algorithm is proposed to solve the POD problem.

5.1. The DBS placement problem

We try to find the best horizontal positions [23] and vertical positions for all DBSs for a given UE association, and the bandwidth and power assignment in the tier-2 backhaul links and the access links, as expressed in Eq. (9). An algorithm named *Opt-DBS-placement*, based on the exhaustive search method [12], is used to determine the optimal locations of all DBSs such that the throughput of the network is maximized. The details are summarized in *Algorithm* 1. Here, G_0 and G_1 are the objective functions of $\mathscr{P}_0$ and $\mathscr{P}_1$, respectively.

$$\begin{aligned} \mathscr{P}_1 : \max_{\tau_j, h_j} \quad & \sum_i \sum_j \omega_{i,j} d_i \\ s.t.: \quad & \\ & C1 : v_j \in \Lambda_1, \quad \forall j \in \mathcal{B}, j > 1, \\ & C2 : h_j \in \Lambda_2, \quad \forall j \in \mathcal{B}, j > 1. \end{aligned} \tag{9}$$

Algorithm 1: Opt-DBS-placement

Input : $\Lambda_1, \Lambda_2, \tilde{f}_j, \tilde{P}_j, \tilde{\omega}_{i,j}, \tilde{p}_{i,j}$, and $\tilde{b}_{i,j}$;
Output: $\tilde{\tau}_j^*$ and $\tilde{h}_j^*$;

```
for τ̃_j ∈ Λ_1 do
    for h̃_j ∈ Λ_2 do
        calculate ω_{i,j}, p_{i,j} and b_{i,j};
        obtain G_1(τ̃_j, h̃_j) = G_0|_{τ_j=τ̃_j, h_j=h̃_j};
get (τ̃*_j, h̃*_j) = argmax_{τ̃_j, h̃_j} G_1(τ̃_j, h̃_j).
```

Theorem 1. *The optimal locations of DBSs, $(\tilde{\tau}_j^*, \tilde{h}_j^*)$, are achieved by Algorithm 1 through exhaustive search for given $\tilde{f}_j$, $\tilde{P}_j$, $\tilde{\omega}_{i,j}$, $\tilde{p}_{i,j}$, and $\tilde{b}_{i,j}$.*

Proof. $(\tilde{\tau}_j^*, \tilde{h}_j^*)$ is the output of *Algorithm* 1, and $(\tilde{\tau}_j^*, \tilde{h}_j^*) = \underset{\tilde{\tau}_j, \tilde{h}_j}{\operatorname{argmax}}\, G_1(\tilde{\tau}_j, \tilde{h}_j) = \underset{\tilde{\tau}_j, \tilde{h}_j}{\operatorname{argmax}}\, G_0\Big|_{\tau_j=\tilde{\tau}_j, h_j=\tilde{h}_j}$. G_0 is the objective function of $\mathscr{P}_0$. Then, $G_0(\tilde{\tau}_j^*, \tilde{h}_j^*) = G_0\Big|_{\tau_j=\tilde{\tau}_j^*, h_j=\tilde{h}_j^*}$. Here, $(\tilde{\tau}_j^*, \tilde{h}_j^*) = \underset{\tau_j, h_j}{\operatorname{argmax}} \sum_i \sum_j \omega_{i,j} d_i$ (the best candidate positions of DBSs are obtained with the maximum throughput of the network). Thus, the optimal $(\tilde{\tau}_j^*, \tilde{h}_j^*)$ is obtained. □

5.2. The BEAT problem

For the tier-2 backhaul, we assume the power of the MDBS allocated to a tier-2 backhaul link is proportional to its bandwidth allocation, i.e., $P_j = f_j z_1$ and z_1 is the power spectrum efficiency of the MDBS ($z_1 = P_1^{max}/f^{max}$). Then, the BEAT problem is formulated as $\mathscr{P}_2$. Let $S_{i,j}$ be the spectrum efficiency $((bit/s)/Hz)$ of the ith UE towards the jth BS, as shown in Eq. (11). Here, UE 1 is associated with the DBS if $S_{1,2} > S_{1,1}$.

$$\begin{aligned} \mathscr{P}_2 : \max_{f_j, P_j} \quad & \sum_i \sum_j \omega_{i,j} d_i \\ s.t.: \quad & \\ & C1 : \sum_i \omega_{i,j} b_{i,j} \le f_j, \quad \forall i \in \mathcal{U}, j \in \mathcal{B}, \\ & C2 : \sum_i \sum_j \omega_{i,j} b_{i,j} \le f^{max}. \end{aligned} \tag{10}$$

$$S_{i,j} = \begin{cases} log_2(1 + s_{i,j}), & \forall i \in \mathcal{U}, j = 0 \\ \min(\xi_j, r_{i,j})/\tilde{b}_{i,j}, & \forall i \in \mathcal{U}, j \in \mathcal{B}, j \ge 1. \end{cases} \tag{11}$$

Let $G_2(\tilde{f}_j, \tilde{P}_j) = G_0\Big|_{f_j=\tilde{f}_j, P_j=\tilde{P}_j}$ be the objective function of problem $\mathscr{P}_2$. Here, $\tilde{f}_j$ and $\tilde{P}_j$ are the total available bandwidth in terms of SCs and total available power of the jth BS, respectively. The optimal backhaul bandwidth and power assignment strategy (*opt-BEAT*) is summarized in *Algorithm* 2.

Algorithm 2: Opt-BEAT

Input : $\tilde{\tau}_j, \tilde{h}_j, f^{max}$ and P_j^{max};
Output: f_j^* and P_j^*;

```
for i ∈ R do
    for j ∈ B do
        calculate S_{i,j};
    obtain S̃_{i,j*} = max(S_{i,j}) and j* = argmax_j S_{i,j};
    ω_{i,j*} = 1;
set ĩ as a descending order of i by S̃_{i,j*};
for ĩ ∈ R do
    calculate f_j = Σ_i ω_{i,j} / Σ_i Σ_j ω_{i,j} and P_j = f_j z_j;
    obtain G_2(f̃_j, P̃_j) = G_0|_{f_j=f̃_j, P_j=P̃_j};
get (f̃*_j, P̃*_j) = argmax_{f_j, P_j} G_2(f̃_j, P̃_j).
```

Theorem 2. *Algorithm 2 achieves the optimal tier-2 backhaul bandwidth and power assignment (f_j^*, P_j^*) for given locations of all DBSs ($\tilde{\tau}_j$, $\tilde{h}_j$) and given radio resources (f^{max}, P_j^{max}).*

Proof. According to Algorithm 2, the maximum spectrum efficiency of each UE is determined by $S^*_{i,j} = \max(S_{i,j})$. The maximum spectrum efficiency strategy is employed to expend the minimum radio resource in provisioning UEs, and thus the same radio resource can serve more UEs. In Step 8, we use the number of UEs instead of the exact total data rate requirement to approximate the bandwidth requirement of each BS. Since the UE data rate requirements are randomly generated, the number of UEs associated to a BS is proportional to the total data rate requirement of UEs. Assume $\tilde{f}^*_j$, $\tilde{P}^*_j$ are the output of *Algorithm* 2. Then, $G_2(\tilde{f}^*_j, \tilde{P}^*_j) = G_0\Big|_{f_j=\tilde{f}^*_j, P_j=\tilde{P}^*_j}$ and $(\tilde{f}^*_j, \tilde{P}^*_j) = \underset{f_j,P_j}{\operatorname{argmax}}\, G_2(\tilde{f}_j, \tilde{P}_j)$. Thus, the best bandwidth and power assignment $(\tilde{f}^*_j, \tilde{P}^*_j)$ for the tier-2 backhaul is achieved. □

$$
\begin{aligned}
\mathscr{P}_3 : \max_{\omega_{i,j}} \quad & \sum_i \sum_j \omega_{i,j} d_i \\
s.t.: \quad & \\
& C1 : \sum_j \omega_{i,j} \leq 1, \quad \forall i \in \mathcal{U}, \\
& C2 : \sum_i \omega_{i,j} p_{i,j} \leq \tilde{P}_j, \quad \forall i \in \mathcal{U}, j \in \mathcal{B}, \\
& C3 : \sum_i \omega_{i,j} d_i \leq \xi_j, \quad \forall i \in \mathcal{U}, j \in \mathcal{B}, j \geq 1 \\
& C4 : \omega_{i,j} \in \{0, 1\}, \quad \forall i \in \mathcal{U}, j \in \mathcal{B}.
\end{aligned} \tag{12}
$$

5.3. The JUNE Problem

Cvijetic *et al.* [24] experimentally demonstrated 100 *Gbps* per channel FSO transmission for $1 - 1.5$ *km*; Liu *et al.* [25] demonstrated 128 *Gbps* FSO over 1 *km* transmission on a simulated atmosphere channel with adjusted turbulence intensity. Thus, constraint $C9$ of problem $\mathscr{P}_0$ is relaxed. Assuming the power of a DBS assigned to a UE is proportional to its assigned bandwidth, i.e., $p_{i,j} = \tilde{b}_{i,j} z^k_j = b_0 b_{i,j} z^k_j$ and $z^k_j = \tilde{\alpha}_j / (b_0 \tilde{f}_j)$. Here, $\tilde{\alpha}_j$ is the total available power in the jth DBS and k is the loop index. Then, $C2$ and $C3$ of problem $\mathscr{P}_0$ are resolved by problem $\mathscr{P}_2$ and $C5$ of problem $\mathscr{P}_0$ is transformed into C2 of problem $\mathscr{P}_3$. Since the DBS placement ($\tilde{\tau}_j$ and $\tilde{h}_j$) and backhaul bandwidth and power ($\tilde{f}_j$ and $\tilde{P}_j$) are determined, the JUNE problem can be formulated as problem $\mathscr{P}_3$. Here, $\tilde{P}_1 = b_0 \tilde{f}_1 z^k_1$, $\tilde{P}_j = P^{max}_j$ and $j > 1$.

We employ an approximate method to solve problem $\mathscr{P}_3$ by adjusting the total available power ($\tilde{P}_j$) of a DBS to relax $C3$. In the kth iteration ($k \geq 1$), $\tilde{P}_j$ is replaced by $\tilde{\alpha}_j$ ($\tilde{\alpha}_j = \sum_k \tilde{\alpha}^k_j$, $\tilde{\alpha}^k_j = \frac{\tilde{K}}{2^k} \tilde{P}_j$, $j > 1$, and $\tilde{\alpha}_1 = \tilde{P}_1$), $\tilde{\alpha}_j$ is the total available power in the jth DBS, $\tilde{\alpha}^k_j$ is the power increment in the kth iteration, and $\tilde{K}$ is the indicator of $C3$ of problem $\mathscr{P}_3$ (it is "1" if $C3$ is satisfied in the kth iteration; otherwise it is "-1"). Then, problem $\mathscr{P}_3$ is transformed into problem $\mathscr{P}_4$, as expressed in Eq. (13). Let $G_3(\omega_{i,j})$ and $G_4(\omega_{i,j}, \alpha_j)$ be the objective functions of problem $\mathscr{P}_3$ and $\mathscr{P}_4$, $G_3(\omega_{i,j}) = G_4\Big|_{\alpha_j = P^{max}_j}$.

Theorem 3. *Assume* $\{\breve{\omega}_{i,j}\}$ *is a solution of problem* $\mathscr{P}_4$. *If* $G_4(\breve{\omega}_{i,j}, \tilde{\alpha}_j) > \epsilon G_4(\omega^*_{i,j}, \tilde{\alpha}_j)$, *then* $G_4(\breve{\omega}_{i,j}, \tilde{\alpha}_j) > \epsilon(1 - \frac{1}{2^k}) G_3(\omega^*_{i,j})$. *Here,* $0 \leq \epsilon \leq 1$.

Proof. Since we use $\tilde{\alpha}^k_j$ to relax $C3$ of problem $\mathscr{P}_3$, more iterations lead to a more accurate result to problem $\mathscr{P}_3$ (the total data rate of a DBS is closer to that of its tier-2 backhaul). The variance between P^{max}_j and $\tilde{\alpha}_j$ is calculated as follows. $P^{max}_j - \tilde{\alpha}_j = P^{max}_j - \sum_k \tilde{\alpha}^k_j = P^{max}_j - \sum_k \frac{\tilde{K}}{2^k} \tilde{P}_j = P^{max}_j - \sum_k \frac{\tilde{K}}{2^k} P^{max}_j \leq (1 - \sum_k \frac{1}{2^k}) P^{max}_j = [1 - (1 - \frac{1}{2^k})] P^{max}_j = \frac{1}{2^k} P^{max}_j$. Then, $\tilde{\alpha}_j \geq (1 - \frac{1}{2^k}) P^{max}_j$. Note that $\tilde{G}_4(\cdot)$ is a linear function of $\tilde{\alpha}_j$. Thus, $G_4(\omega_{i,j}, \tilde{\alpha}_j) \geq (1 - \frac{1}{2^k}) G_4(\omega_{i,j}, P^{max}_j)$. Since $G_3(\omega_{i,j}) = G_4\Big|_{\alpha_j = P^{max}_j}$, we have $G_4(\omega_{i,j}, \tilde{\alpha}_j) \geq (1 - \frac{1}{2^k}) G_3(\omega_{i,j})$ and $G_4(\omega^*_{i,j}, \tilde{\alpha}_j) \geq (1 - \frac{1}{2^k}) G_3(\omega^*_{i,j})$. If we have $G_4(\breve{\omega}_{i,j}, \tilde{\alpha}_j) \geq \epsilon G_4(\omega^*_{i,j}, \tilde{\alpha}_j)$, then $G_4(\breve{\omega}_{i,j}, \tilde{\alpha}_j) \geq \epsilon(1 - \frac{1}{2^k}) G_3(\omega^*_{i,j})$. □

$$
\begin{aligned}
\mathscr{P}_4 : \max_{\omega_{i,j}} \quad & \sum_i \sum_j \omega_{i,j} d_i \\
s.t.: \quad & \\
& C1 : \sum_j \omega_{i,j} \leq 1, \quad \forall i \in \mathcal{U}, \\
& C2 : \sum_i \omega_{i,j} p_{i,j} \leq \tilde{\alpha}_j, \quad \forall i \in \mathcal{U}, j \in \mathcal{B}, j > 1, \\
& C3 : \omega_{i,j} \in \{0, 1\}, \quad \forall i \in \mathcal{U}, j \in \mathcal{B}, j > 1.
\end{aligned} \tag{13}
$$

$$
\begin{aligned}
\mathscr{P}_5 : \max_{\omega_{i,j}} \quad & \sum_i \sum_j \omega_{i,j} d_i \\
s.t.: \quad & \\
& C1, C2 \quad in \quad Eq.(13) \\
& C3 : 0 \leq \omega_{i,j} \leq 1, \quad \forall i \in \mathcal{U}, j \in \mathcal{B}.
\end{aligned} \tag{14}
$$

We propose an approximation algorithm, named Approximation Algorithm for JUNE (*AA-JUNE*), as expressed in Algorithm 3, to solve problem $\mathscr{P}_4$ for given $\tilde{\alpha}_j$ ($j \in \mathcal{B}$ and $j > 1$) and $\tilde{\alpha}^k_j$. We first calculate the weight $\varsigma_{i,\tilde{j}}$ (*Steps* $1 - 6$), which is used to determine the UE association. Then, all UEs are put in descending order of $\tilde{i}$ by the weight (*Step* 7). After that, one solution $\tilde{\mathcal{U}}_1$ (*Steps* $8 - 16$) and another solution $\tilde{\mathcal{U}}_3$ (*Steps* $17 - 19$) are obtained. Finally, the solution ($\tilde{\mathcal{U}}_1$ or $\tilde{\mathcal{U}}_3$) which has the maximum throughput is returned (*Step* 20); $\tilde{p}_{i,j}$ and $\tilde{b}_{i,j}$ are also obtained (*Step* 21). Here, $G_5(\cdot)$ is a function of $\tilde{\omega}_{i,j}$, which represents the total data rate of all served UEs for a given $\tilde{\alpha}_j$, $G_5(\tilde{\omega}_{i,j}) = G_4\Big|_{\omega_{i,j} = \tilde{\omega}_{i,j}, \alpha_j = \tilde{\alpha}_j}$); $\varsigma_{i,\tilde{j}} = d_i / p_{i,\tilde{j}}$ is the weight to determine the UE association; $\tilde{\omega}_{\tilde{i},\tilde{j}}$ is the UE association indicator for the set of UEs in $\tilde{\mathcal{U}}_1$; $\hat{\omega}_{\hat{i},j}$ the UE association indicator for the set of UEs in $\tilde{\mathcal{U}}_3$.

Note that $\omega_{i,j}$ is a binary variable and $\mathscr{P}_4$ can be transformed into $\mathscr{P}_5$ if we relax $\omega_{i,j}$ to a continuous variable ($\omega_{i,j} \in [0, 1]$). Assuming $G_6(\cdot)$ is the objective function of problem $\mathscr{P}_5$. Obviously, the optimal throughput of problem $\mathscr{P}_5$ is bigger or equal to that of problem $\mathscr{P}_4$, viz., $G_6(\omega^*_{i,j}) \geq G_5(\omega^*_{i,j})$.

Theorem 4. *The AA-JUNE algorithm achieves an approximation ratio of* $\frac{1}{2}$ *for solving problem* $\mathscr{P}_4$. *Moreover, the AA-JUNE algorithm achieves the optimal throughput when all UEs are provisioned.*

Algorithm 3: AA-JUNE

Input : $\mathcal{B}, \mathcal{U}, d_i, \tilde{\alpha}_j, \tilde{f}_j, \tilde{P}_j, \tilde{\tau}_j$ and $\tilde{h}_j$;
Output: $\tilde{\omega}_{i,j}, \tilde{b}_{i,j}$ and $\tilde{p}_{i,j}$;

1 $\tilde{i} = 1, \tilde{\mathcal{U}}_1 = \varnothing, \mathcal{U}_2 = \mathcal{U}, \alpha_j = 0, \forall j \in \mathcal{B}$;
2 $z_j^k = \tilde{\alpha}_j / f^{max}, j > 1$;
3 **for** $i \in \mathcal{U}_2$ **do**
4   **for** $j \in \mathcal{B}$ **do**
5   compute $b_{i,j}$ and $p_{i,j}$;
6   obtain $p_{i,\tilde{j}} = \min(p_{i,j})$ and $\tilde{j} = \underset{j}{\operatorname{argmin}}\, p_{i,j}, \forall i$;
7 put i in a descending order of $\tilde{i}$ by $\varsigma_{i,\tilde{j}} = d_i / p_{i,\tilde{j}}$;
8 **while** $\alpha_j \leq \tilde{\alpha}_j$ & $\tilde{\mathcal{U}}_2 \neq \varnothing$ **do**
9   **if** $\alpha_{\tilde{j}} + p_{\tilde{i},\tilde{j}} \leq \tilde{\alpha}_{\tilde{j}}$ **then**
10     $\omega_{\tilde{i},\tilde{j}} = 1$;
11     $\tilde{\mathcal{U}}_2 = \tilde{\mathcal{U}}_2 \setminus \tilde{i}$;
12     $\tilde{\mathcal{U}}_1 = \tilde{\mathcal{U}}_1 \cup \{\tilde{\omega}_{\tilde{i},\tilde{j}}\}$;
13     $\alpha_{\tilde{j}} = \alpha_{\tilde{j}} + p_{\tilde{i},\tilde{j}}$;
14   **else**
15   repeat Steps 2-5;
16   $\tilde{i} = \tilde{i} + 1$;
17 $\hat{i} = 1, \tilde{\mathcal{U}}_3 = \varnothing$;
18 **for** $\hat{i} \leq |\mathcal{B}|$ **do**
19   $\tilde{\mathcal{U}}_3 = \tilde{\mathcal{U}}_3 \cup \{\hat{\omega}_{\hat{i},\hat{j}} = \underset{\omega_{\hat{i},\hat{j}}}{\operatorname{argmax}}\, \omega_{\hat{i},\hat{j}} d_{\hat{i}}\}$;
20 return $\tilde{\mathcal{U}}_1$ or $\tilde{\mathcal{U}}_3$ with a higher throughput;
21 obtain $\tilde{b}_{i,j}$ and $\tilde{p}_{i,j}$.

Algorithm 4: AA-POD

Input : $\mathcal{B}, \mathcal{U}, d_i, f_j^{max}, P^{max}$;
Output: $\tilde{\omega}_{i,j}, \tilde{b}_{i,j}, \tilde{p}_{i,j}, \tilde{f}_j, \tilde{P}_j, \tilde{\tau}_j$ and $\tilde{h}_j$;

1 **for** $\tilde{\tau}_j \in \Lambda_1$ **do**
2   **for** $\tilde{h}_j \in \Lambda_2$ **do**
3   obtain $\tilde{f}_j$ and $\tilde{P}_j$ by *Algorithm* 2;
4     $\hat{\beta} = |\mathcal{B}| - 1, k_j = 1, j \in \mathcal{B}, j > 1$;
5   **while** $\hat{\beta} > 0$ & $k_j \leq k^{max}$ **do**
6       $\tilde{\omega}_{i,j} = 0, \tilde{b}_{i,j} = 0, \tilde{p}_{i,j} = 0$, and $\hat{\beta} = |\mathcal{B}| - 1$;
7   **for** $j \in \mathcal{B}, j > 1$ **do**
8   **if** $|\frac{(\xi_j - \sum_i \tilde{\omega}_{i,j} d_i)}{\xi_j}| \leq \beta_0$ **then**
9           $\hat{\beta} = \hat{\beta} - 1$;
10           $\tilde{\alpha}_j^{k_j} = 0$;
11   **else if** $\frac{(\xi_j - \sum_i \tilde{\omega}_{i,j} d_i)}{\xi_j} > \beta_0$ **then**
12           $\hat{\beta}_j = 1$ and $\tilde{\alpha}_j^{k_j} = \frac{\hat{\beta}_j}{2^k} \tilde{P}_j$;
13   **else**
14           $\hat{\beta}_j = -1$ and $\tilde{\alpha}_j^{k_j} = \frac{\hat{\beta}_j}{2^k} \tilde{P}_j$;
15         $\tilde{\alpha}_j = \sum_{k_j} \tilde{\alpha}_j^{k_j}$;
16   obtain $\max(G_5(\tilde{\omega}_{\tilde{i},\tilde{j}}), G_5(\hat{\omega}_{\hat{i},\hat{j}}))$ by *Algorithm* 3;
17   calculate $\tilde{\omega}_{i,j}, \tilde{b}_{i,j}$ and $\tilde{p}_{i,j}$;
18 get $(\tilde{\tau}_j^*, \tilde{h}_j^*) = \underset{\tau_j, h_j}{\operatorname{argmax}}\, G_1(\tilde{\tau}_j, \tilde{h}_j)$.

Proof. Here, two scenarios are considered: no UE blocked and one or more UEs are blocked.

1) No UE blocked scenario (all UEs are served). Let $G_5(\omega_{i,j}^*)$ be the optimal throughput of $\mathscr{P}_4$, and $G_6(\omega_{i,j}^*)$ be the optimal throughput of $\mathscr{P}_5$ ($p_{i,j}^*$, $b_{i,j}^*$ depend on $\omega_{i,j}^*$). We can calculate the total throughput by the AA-JUNE algorithm for $\mathscr{P}_4$ and $\mathscr{P}_5$ as follows. $\max(G_5(\tilde{\omega}_{\tilde{i},\tilde{j}}), G_5(\hat{\omega}_{\hat{i},\hat{j}})) = G_5(\tilde{\omega}_{\tilde{i},\tilde{j}}) = \sum_i \sum_j \tilde{\omega}_{\tilde{i},\tilde{j}} d_i = \sum_i (\sum_j \tilde{\omega}_{\tilde{i},\tilde{j}}) d_i = \sum_i d_i$, $G_5(\omega_{i,j}^*) = \sum_i \sum_j \omega_{i,j}^* r_i = \sum_i d_i$, and $G_6(\omega_{i,j}^*) = \sum_i \sum_j \bar{\omega}_{i,j}^* r_i = \sum_i d_i$. Here, $\sum_j \tilde{\omega}_{\tilde{i},\tilde{j}} = 1$, $\sum_j \omega_{i,j}^* = 1$, $\sum_j \bar{\omega}_{i,j}^* = 1$, $\tilde{\omega}_{\tilde{i},\tilde{j}} \in \tilde{\mathcal{U}}_1$ and $\hat{\omega}_{\hat{i},\hat{j}} \in \tilde{\mathcal{U}}_3$. Then, $\max(G_5(\tilde{\omega}_{\tilde{i},\tilde{j}}), G_5(\hat{\omega}_{\hat{i},\hat{j}})) = G_5(\omega_{i,j}^*) = G_6(\omega_{i,j}^*)$. The AA-JUNE algorithm achieves the optimal throughput for both $\mathscr{P}_4$ and $\mathscr{P}_5$.

2) One or more UEs blocked scenario (not all UEs are provisioned). Assume υ is the index of the first blocked UEs by the AA-JUNE algorithm. Since all UEs are provisioned according to the order of the ratio of the data rate to the required power, viz., $\frac{d_1}{p_{1,\tilde{j}_1}} \geq \frac{d_2}{p_{2,\tilde{j}_2}} \geq \cdots \geq \frac{d_{\tilde{i}}}{p_{\tilde{i},\tilde{j}_{\tilde{i}}}}$, then $G_6(\omega_{i,j}^*) = G_5(\cup_{\tilde{i}=1}^{\upsilon-1} \tilde{\omega}_{(\upsilon-1),\tilde{j}_{(\upsilon-1)}}) + G_5(\cup_{\tilde{i}=1}^{\upsilon+|\mathcal{B}|-1} \delta_\upsilon \tilde{\omega}_{\upsilon,j_\upsilon})$. Here, $\tilde{\mathcal{U}}_1 = \cup_{\tilde{i}=1}^{\upsilon-1} \tilde{\omega}_{(\upsilon-1),\tilde{j}_{(\upsilon-1)}}$, $\tilde{\omega}_{\upsilon,j_\upsilon} = \underset{\tilde{\omega}_{\tilde{i},\tilde{j}}}{\operatorname{argmax}}\, \tilde{\omega}_{\tilde{i},\tilde{j}} d_i$, $\delta_\upsilon = (\tilde{\alpha}_{j_\upsilon} - \sum_{\tilde{i}} \tilde{\omega}_{\tilde{i},\tilde{j}} \tilde{p}_{\tilde{i},\tilde{j}}) / (\tilde{\omega}_{\upsilon,j_\upsilon} \tilde{p}_{\upsilon,j_\upsilon})$, $\delta_\upsilon \in [0,1)$, $\tilde{i} \in \mathcal{U} \setminus \mathcal{U}_1$, and $j_\upsilon = 1, 2, \cdots, |\mathcal{B}|$. Meanwhile, $G_5(\hat{\omega}_{\hat{i},\hat{j}}) \geq G_5(\cup_{\tilde{i}=1}^{\upsilon+|\mathcal{B}|-1} \delta_\upsilon \tilde{\omega}_{\upsilon,j_\upsilon})$, $\hat{\omega}_{\hat{i},\hat{j}} \in \tilde{\mathcal{U}}_3$. This is because $\tilde{\omega}_{\upsilon,j_\upsilon}$ is the UE association indicator, which represents the maximum throughput among the υth UE to the last UE; $\hat{\omega}_{\hat{i},\hat{j}}$ is the UE association indicator, which represents the maximum throughput among all UEs. Thus, $G_6(\omega_{i,j}^*) < G_5(\cup_{\tilde{i}=1}^{\upsilon-1} \tilde{\omega}_{(\upsilon-1),\tilde{j}}) + G_5(\hat{\omega}_{\hat{i},\hat{j}})$ and $G_6(\omega_{i,j}^*) < G_5(\tilde{\mathcal{U}}_1) + G_5(\tilde{\mathcal{U}}_3)$. Note that $G_5(\omega_{i,j}^*) \leq G_6(\omega_{i,j}^*)$. Thus, $G_5(\omega_{i,j}^*) < G_5(\cup_{\tilde{i}=1}^{\upsilon-1} \tilde{\omega}_{(\upsilon-1),\tilde{j}}) + G_5(\hat{\omega}_{\hat{i},\hat{j}})$ and $G_5(\omega_{i,j}^*) < G_5(\tilde{\mathcal{U}}_1) + G_5(\tilde{\mathcal{U}}_3)$. Then, $G_5(\tilde{\mathcal{U}}_1) > \frac{1}{2} G_5(\omega_{i,j}^*)$ or $G_5(\tilde{\mathcal{U}}_3) > \frac{1}{2} G_5(\omega_{i,j}^*)$. Hence, $\max(G_5(\tilde{\mathcal{U}}_1), G_5(\tilde{\mathcal{U}}_3)) > \frac{1}{2} G_5(\omega_{i,j}^*)$, Algorithm 3 achieves at least $\frac{1}{2}$ of the optimal throughput of $\mathscr{P}_4$. In other words, Algorithm 3 has a $\frac{1}{2}$ approximation ratio and its lower bound is $\frac{1}{2}$ of the optimal throughput of $\mathscr{P}_4$. □

5.4. The POD Problem

Here, we solve the POD problem based on the solution for the sub-problems. An approximation algorithm, named *AA-POD*, is proposed to solve the POD problem, as delineated in *Algorithm* 4. First, the bandwidth and power of the tier-2 backhaul links ($\tilde{P}_j$ and $\tilde{f}_j$) is obtained (*Step* 3). Second, the total available power ($\tilde{\alpha}_j$) of each DBS is computed (*Steps* 5 – 15). Third, the UE association, bandwidth and power assignment ($\tilde{\omega}_{i,j}$, $\tilde{p}_{i,j}$ and $\tilde{b}_{i,j}$) are obtained by *Algorithm* 3 (*Steps* 16 – 17). Finally, the horizontal positions and vertical positions ($\tilde{\tau}_j^*$ and $\tilde{h}_j^*$) are determined (*Step* 18).

Theorem 5. *The AA-POD algorithm achieves an approximation ratio of* $\frac{1}{2}(1 - \frac{1}{2^k})$ *for solving problem* $\mathscr{P}_0$. *Here, k is the number of iterations.*

Proof. Since the AA-POD algorithm is designed based on *Algorithm* 1, *Algorithm* 2 and *Algorithm* 3, the AA-POD algorithm can be concluded with an approximation ratio of $\frac{1}{2}(1 - \frac{1}{2^k})$. Moreover, the AA-POD algorithm achieves the optimal throughput which is equivalent to problem $\mathscr{P}_0$ when all UEs are provisioned. □

Table 2: Parameters for Simulations

$\lvert\mathcal{B}\rvert$	4 (including three DBSs)
$\lvert\mathcal{U}\rvert$	$\{40, 45, \cdots, 75\}$
(a, b)	$(9.61, 0.16)$
(η_1^L, η_2^L), LoS path loss of BS-UE	$(103.8, 20.9)dB$ [19]
(η_1^N, η_2^N), NLoS path loss of BS-UE	$(145.4, 37.5)dB$ [19]
f_0	2 GHz
coverage area of the HetNet	$1000m \times 1000m$
$h_j, \forall j \in \mathcal{B}, j > 1$	$\{40, 60, \cdots, 200\}$ m
N_0	$-174\ dBm/Hz$
$\tilde{\beta}_{SI}$	130 dB [9]
d_i	$\{1, 2, 4, 6\}\ Mbps$
$P_j^{max}, \forall j \in \mathcal{B}$	1 W
f^{max}	100 SCs
b_0	180 kHz
k^{max}	14
β_0	0.0001

6. Performance Evaluation

MATLAB is utilized for the evaluation, and we run the simulations for 200 times to achieve average results. The coverage of the HetNet is $1000m \times 1000m$, and this area is divided into 36 equal sub-areas, which are the candidate horizontal locations to place DBSs. All DBSs are placed at the same altitude. The altitude of the MDBS is set at $50m$, and it is hovering at the center on the coverage area. The total bandwidth in the OFDMA network is 20 MHz. The Matérn cluster process is utilized to generate the UE traffic, while the Possion Process is employed to generate the parent points, and a uniform distribution is leveraged to generate the daughter poings (UEs) surrounding the parent points [18]. All simulation parameters are listed in Table 2.

Two baseline algorithms are utilized to contrast the performance of the AA-POD algorithm. One is the Dynamic-DSP in [26] algorithm with fixed bandwidth and power assignment ($\tilde{f}_j = f^{max}/|\mathcal{B}|$) in the tier-2 backhaul (*DDSP-Fixed*), which obtains the $|\mathcal{B}|$ locations with the maximum weight for all DBSs, and the weight is determined by the number of UEs and the locations of UEs [26]. For the DDSP-Fixed algorithm, the UE association is determined by the best SINR strategy. The other baseline algorithm utilizes half-duplex DBSs with fixed bandwidth and power assignment in the tier-2 backhaul (*HD-Fixed*), which is exactly the same as the DDSP-Fixed algorithm, but with the total available bandwidth capacity of the tier-2 backhaul link and the access link half of those of the DDSP-Fixed algorithm.

The results of the total throughput of the network versus different altitudes with 75 UEs are shown in Fig. 2. The total throughput of the AA-POD algorithm and that of the DDSP-Fixed algorithm increase when the altitude increases because access links of DBSs achieve high data rate as the backhaul interference decreases. The total throughput of the HD-Fixed algorithm increases when the altitude is smaller than 80m, owing to the bottleneck of the access links (the NLOS path loss decreases as the altitude increases and thus results in an increase of an access link's data rate); and then the total throughput decreases when the altitude is higher than 80m, owing to the bottleneck of the tier-2 backhaul links (the path loss of a tier-2

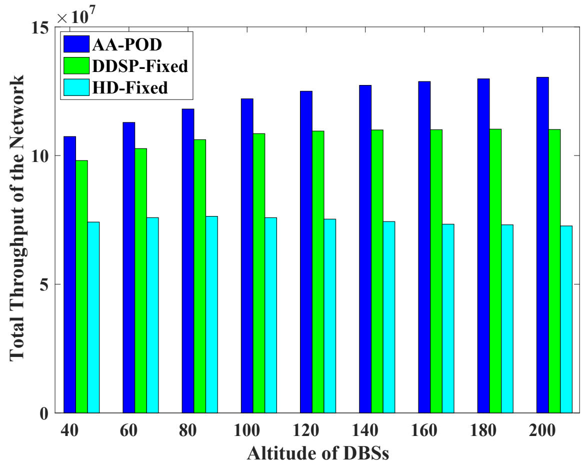

Figure 2: Total throughput versus altitude with 85 UEs.

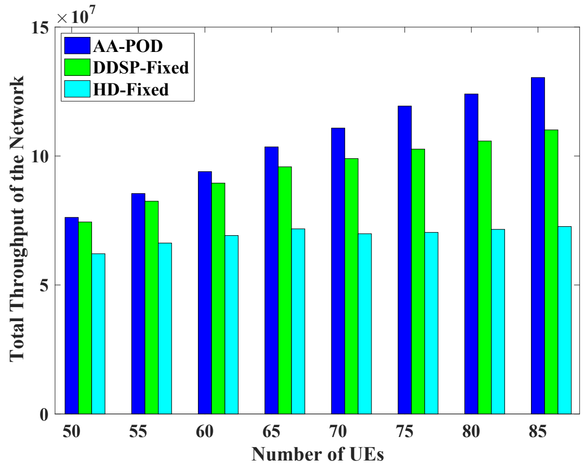

Figure 3: Total throughput versus the number of UEs at 200m altitude.

backhaul link increases as the altitude increases and thus results in a decrease of the data rate). Note that for the HD-Fixed algorithm, the total bandwidth (f_j) assigned to a DBS needs to be equally split in a tier-2 backhaul link ($\frac{f_j}{2}$) and its access link ($\frac{f_j}{2}$) while the total bandwidth (f_j) can be reused in the tier-2 backhaul link and its access link of the other two algorithms with FD-enabled DBSs.

Fig. 3 shows the total throughput performance versus the number of UEs at 200m altitude. The total throughput of all algorithms increase as the number of UEs increases. This is because each BS has more flexibility to select the UEs with better SINR when the number of UEs increases (less radio resources is required to provision the same number of UEs), implying that the total throughput increases as the number of UE increases. The total throughput of the AA-POD algorithm is superior to that of the DDSP-Fixed algorithm and that of the HD-Fixed algorithm, by up to 18.5% and 79.5% improvement, respectively. The AA-POD algorithm has better performance than the HD-Fixed algorithm because the FD-enabled DBSs are used. The AA-POD algorithm has better performance than the DDSP-Fixed algorithm because the former has re-assigned the total bandwidth and power in the tier-2 backhaul links and in-

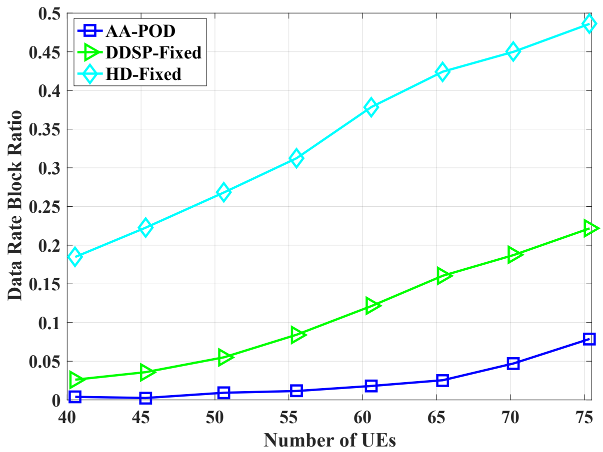

Figure 4: Data rate block ratio at 200m altitude.

corporated better positions for all DBSs.

The results of the data rate block ratio versus the number of UEs at 200m altitude are shown in Fig. 4. The data rate block ratio is the total data rate requirement of provisioned UEs to the total data rate requirement of all UEs ($\sum_i \sum_j \omega_{i,j} d_i / (\sum_i d_i)$). The data rate block ratio becomes higher when the number of UEs increases, and the DDSP-Fixed algorithm performs better than the HD-Fixed algorithm because FD-enabled DBSs are utilized. The AA-POD algorithm achieves the lowest data rate block ratio and no UEs are blocked until the number of UEs reaches 50. This is attributed to the efficient bandwidth and power assignment of the tier-2 backhaul, the efficient bandwidth and power assignment of all UEs, and the optimal positions of all DBSs.

7. Conclusion

We have proposed an IBFD enabled DBS-aided HetNet framework with free space optics in the tier-1 backhaul and flexible bandwidth and power assignment in the tier-2 backhaul for the next generation wireless networks, and then formulated the problem of Placement and cOmmunications in the DBS-aided HetNet (*POD*). The POD problem is decomposed into three sub-problems, which can be solved by respective approximation algorithms sequentially. Then, the AA-POD algorithm is proposed to solve the POD problem, and it is proved to have an approximation ratio of $\frac{1}{2}(1 - \frac{1}{2^k})$ (k is the number of loops) and to achieve the optimal positions of all DBSs and the optimal bandwidth and power assignment in the tier-2 backhaul. Evaluation results have demonstrated that the AA-POD algorithm is superior to two baseline algorithms by providing up to 18.5% and 79.5% throughput improvement, respectively.

References

[1] DOCOMO, DOCOMO 5G White Paper, https://www.nttdocomo.co.jp/english (July 2014).

[2] X. Sun, N. Ansari, Edgeiot: Mobile edge computing for the internet of things, IEEE Commun. Mag. 54 (12) (2016) 22–29.

[3] L. Zhang *et al.*, A survey of advanced techniques for spectrum sharing in 5G networks, IEEE Wireless Commun. 24 (5) (2017) 44–51.

[4] L. Zhang, N. Ansari, A framework for 5G networks with in-band full-duplex enabled drone-mounted base-stations, IEEE Wireless Commun., doi: 10.1109/MWC.2019.1800486.

[5] S. Sekander, H. Tabassum, E. Hossain, Multi-tier drone architecture for 5G/B5G cellular networks: challenges, trends, and prospects, IEEE Commun. Mag. 56 (3) (2018) 96–103.

[6] I. Bor-Yaliniz, H. Yanikomeroglu, The new frontier in RAN heterogeneity: Multi-tier drone-cells, IEEE Commun. Mag. 54 (11) (2016) 48–55.

[7] L. Zhang, N. Ansari, Approximate algorithms for 3-d placement of ibfd enabled drone-mounted base-stations, IEEE Trans. Veh. Technol., doi: 10.1109/TVT.2019.2923143.

[8] C. D. Nwankwo *et al.*, A survey of self-interference management techniques for single frequency full duplex systems, IEEE Access 6 (2018) 30242–30268.

[9] Y. S. Choi, H. Shirani-Mehr, Simultaneous transmission and reception: Algorithm, design and system level performance, IEEE Trans. on Wireless Commun. 12 (12) (2013) 5992–6010.

[10] D. Bharadia, E. M. S. Katti, Full duplex radios, in: ACM SIGCOMM, 2013, pp. 375–386.

[11] A. Al-Hourani, S. Kandeepan, S. Lardner, Optimal LAP altitude for maximum coverage, IEEE Wireless Comm. Lett. 3 (6) (2014) 569–572.

[12] M. Alzenad, A. El-Keyi, H. Yanikomeroglu, 3-D placement of an unmanned aerial vehicle base station for maximum coverage of users with different QoS requirements, IEEE Wireless Comm. Lett. 7 (1) (2018) 38–41.

[13] H. Zhao *et al.*, Deployment algorithms for UAV airborne networks toward on-demand coverage, IEEE J. Sel. Areas Commun. 36 (9) (2018) 2015–2031.

[14] C. Nam, C. Joo, S. Bahk, Joint subcarrier assignment and power allocation in full-duplex OFDMA networks, IEEE Trans. on Wireless Commun. 14 (6) (2015) 3108–3119.

[15] G. Yu *et al.*, Ultra-dense heterogeneous networks with full-duplex small cell base stations, IEEE Network 31 (6) (2017) 108–114.

[16] U. Siddique, H. Tabassum, E. Hossain, Downlink spectrum allocation for in-band and out-band wireless backhauling of full-duplex small cells, IEEE Trans. Commun. 65 (8) (2017) 3538–3554.

[17] A. Sharma, R. K. Ganti, J. K. Milleth, Joint backhaul-access analysis of full duplex self-backhauling heterogeneous networks, IEEE Trans. on Wireless Commun. 16 (3) (2017) 1727–1740.

[18] L. Zhang, N. Ansari, On the number and 3-D placement of in-band full-duplex enabled drone-mounted base-stations, IEEE Wireless Comm. Lett. 8 (1) (2019) 221–224.

[19] 3GPP TR 36.828 version 11.0.0, release 11, 3GPP Tech. Rep., 2012. URL http://www.qtc.jp/3GPP/Specs/36828-b00.pdf

[20] Q. Fan, N. Ansari, Towards traffic load balancing in drone-assisted communications for IoT, IEEE Internet of Things Journal 6 (2) (2019) 3633–3640.

[21] M. S. Elbamby *et al.*, Resource optimization and power allocation in in-band full duplex-enabled non-orthogonal multiple access networks, IEEE J. Sel. Areas Commun. 35 (12) (2017) 2860–2873.

[22] L. Fleischer *et al.*, Tight approximation algorithms for maximum general assignment problems, in: Proceedings of the 17th Annual ACM-SIAM Symposium on Discrete Algorithms, 2006, pp. 611–620.

[23] X. Guo *et al.*, Robust WiFi localization by fusing derivative fingerprints of rss and multiple classifiers, IEEE Trans Ind. Informat., doi: 10.1109/TII.2019.2910664.

[24] N. Cvijetic *et al.*, 100 Gb/s per-channel free-space optical transmission with coherent detection and MIMO processing, in: Proc. of ECOC, 2009, pp. 1–2.

[25] X. Liu *et al.*, 128 Gbit/s free-space laser transmission performance in a simulated atmosphere channel with adjusted turbulence, IEEE Photonics Journal 10 (2) (2018) 1–10.

[26] L. Zhang, Q. Fan, N. Ansari, 3-D drone-base-station placement with in-band full-duplex communications, IEEE Comm. Lett. 22 (9) (2018) 1902–1905.